X-Ray Attenuation-Coefficient Measurements*

J. H. McCrary, Elizabeth H. Plassmann, J. M. Puckett, A. L. Conner, and G. W. Zimmermann
University of California, Los Alamos Scientific Laboratory, Los Alamos, New Mexico
(Received 11 July 1966)

X-ray attenuation coefficients were measured in the energy range of 25 keV to 130 keV for the following elements: Be, C, Mg, Al, S, Ti, Fe, Ni, Cu, Zn, Zr, Nb, Mo, Ag, Sn, La, Gd, Hf, W, Au, Pb, Th, U, and Pu. Narrow beam collimation was used with a Bragg diffraction monochromator. Experimental errors were less than 2% for most of the measurements.

INTRODUCTION

ALTHOUGH a large amount of work has been done in measuring and compiling x-ray attenuation coefficients,[1–5] presently available data still contain fairly large errors and inconsistencies in the energy range of 25 to 130 keV. The total attenuation coefficient, μ with units of cm²/gm, is defined by the equation

$$I=I_0e^{-\mu x}, \quad (1)$$

where I_0 is the incident beam intensity, I is the transmitted beam intensity, and x is the sample thickness in gm/cm². In the present work an attempt was made to measure μ precisely in the energy range of 25 to 130 keV for a large number of elements using diffracted x rays and narrow beam geometry.[6]

APPARATUS

Figure 1 is a schematic drawing of the experimental apparatus. The x-ray source was a Machlett Industrial Thermax tube with a window equivalent to 0.040-in. Al and a W target powered by a Picker 150-kV (peak), 10-mA power supply. The collimation system was of the aluminum slot type as described by Cid-Dresdner and Buerger.[7] Each of the three slots was $\frac{1}{32}$ in. square and 6 in. long. The angular resolution for this geometry was thus 5 min of arc. The diffraction grating was a quartz crystal whose exposed plane spacing was 1.3745 Å. Two coaxial dividing heads provided separate control of θ and 2θ with an uncertainty of less than 1 min of arc. The detector was a $\frac{3}{4}$-in.-diam by $\frac{1}{2}$-in.-long NaI(Tl) crystal covered by a 0.005-in. Be foil. The counter was essentially 100% efficient in the energy range of interest. The crystal was mounted on a RCA 6342A photomultiplier tube, the pulses from which were amplified and fed through a single-channel analyzer to a preset time scaler. To eliminate higher order diffracted x rays and to minimize background, the single-channel analyzer was adjusted so that only pulses from photo-electric events in the detector crystal were registered in the scaler. The counting system had a resolving time of 1 μsec. The x-ray tube and the detector were shielded with lead so that the background count ($\frac{1}{4}$-in. lead in diffracted beam) was usually less than 1% of the diffracted beam count.

The collimators and diffraction grating were aligned mechanically to within ± 0.001 in. of their optimum positions. This alignment was checked by observing the characteristic radiations emitted by the tungsten target and by scanning well known K edges of several elements. It was thus determined that the angular resolution was indeed 5 min of arc and that the angles indicated on the θ and 2θ dividing heads had an uncertainty of less than 1 min. It was calculated that the error introduced in μ by this angular (and thus energy) resolution was less than 0.1%. One minute of arc corresponds to 1.1 keV at 130 keV and to 0.040 keV at 25 keV.

SAMPLES

Nonuniformity of samples can introduce large errors in the measured values of μ. In the present work, sample thicknesses varied from 0.0008 to 0.900 in. The thinner samples (with the exception of plutonium) were fabricated in rolling mills. A typical sample from the rolling mill had an area of several square inches.

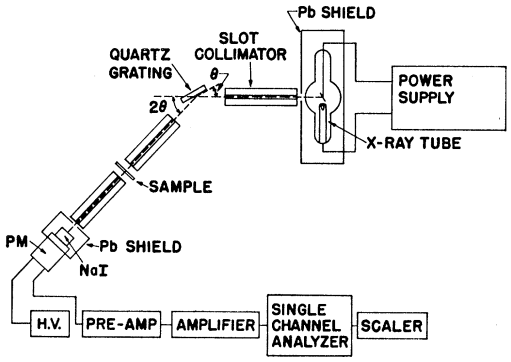

FIG. 1. Schematic diagram of experimental apparatus.

* This work was performed under the auspices of the U. S. Atomic Energy Commission.

[1] G. W. Grodstein, Natl. Bur. Std. (U.S.) Circ. No. 583 (1957).
[2] R. T. McGinnies, Natl. Bur. Std. (U.S.) Circ. No. 583, Suppl. (1959).
[3] H. M. Stainer, U. S. Bur. Mines, Inform. Circ. No. 8166 (1963).
[4] M. Wiedenbeck, Phys. Rev. **126**, 1009 (1962).
[5] C. Weissmantel and M. Wuenschmann, Z. Chem. **5**, 191 (1965).
[6] This work is a presentation of experimental results. The comparison of these results with theory is intended as a future publication.
[7] Hilda Cid-Dresdner and M. J. Buerger, J. Sci. Instr. **41**, 689 (1964).

TABLE I. Experimentally determined values of x-ray attenuation coefficients.

X-ray energy (keV)	Beryllium (cm^2/gm)	Carbon (cm^2/gm)	Magnesium (cm^2/gm)	Aluminum (cm^2/gm)	Sulfur (cm^2/gm)	Titanium (cm^2/gm)
24.00±0.02						
25.00±0.02	0.1780±0.0028	0.2968±0.0018	1.430 ±0.011	1.811 ±0.012	3.109 ±0.045	8.541 ±0.041
26.01±0.02						
28.00±0.02						
30.04±0.03	0.1697±0.0017	0.2466±0.0017	0.8966±0.0056	1.085 ±0.006	2.035 ±0.016	4.992 ±0.016
35.05±0.04						
35.06±0.04						3.246 ±0.015
40.04±0.05	0.1572±0.0010	0.2032±0.0006	0.4734±0.0015	0.5561±0.0044	0.9764±0.0099	2.239 ±0.006
45.01±0.06						
50.08±0.08	0.1520±0.0008	0.1841±0.0006	0.3200±0.0036	0.3517±0.0014	0.5711±0.0031	1.199 ±0.004
55.04±0.10						
60.03±0.12	0.1467±0.0007	0.1715±0.0005	0.2519±0.0021	0.2748±0.0020	0.3975±0.0044	0.7515±0.0020
61.82±0.12						
70.04±0.16	0.1421±0.0008	0.1649±0.0008	0.2139±0.0014	0.2219±0.0014	0.3085±0.0011	0.5252±0.0016
70.20±0.16						
79.96±0.21				0.1970±0.0008	0.2544±0.0013	0.3997±0.0024
80.16±0.22						
84.99±0.23	0.1366±0.0005	0.1549±0.0006	0.1864±0.0012			
89.92±0.26				0.1812±0.0016	0.2253±0.0011	0.3187±0.0019
90.18±0.26						
94.00±0.28						
100.06±0.32	0.1306±0.0007	0.1512±0.0007	0.1658±0.0011	0.1665±0.0008	0.2012±0.0010	0.2670±0.0007
100.38±0.33						
109.99±0.39						0.2297±0.0008
110.39±0.39						
114.87±0.43			0.1567±0.0006	0.1565±0.0010	0.1773±0.0013	
120.21±0.47						0.2050±0.0016
120.67±0.47						
123.09±0.49						
127.11±0.53						
130.31±0.55	0.1229±0.0011	0.1414±0.0010	0.1439±0.0014	0.1463±0.0012	0.1653±0.0022	0.1910±0.0020
131.41±0.55						

X-ray energy (keV)	Iron (cm^2/gm)	Nickel (cm^2/gm)	Copper (cm^2/gm)	Zinc (cm^2/gm)	Zirconium (cm^2/gm)	Niobium (cm^2/gm)
24.00±0.02						
25.00±0.02	13.72 ±0.08	16.93 ±0.10	18.01 ±0.13	19.79 ±0.09	40.83 ±0.21	43.17 ±0.20
26.01±0.02						
28.00±0.02						
30.04±0.03	8.167 ±0.030	10.21 ±0.05	10.84 ±0.05	11.95 ±0.06	25.00 ±0.15	25.92 ±0.10
35.05±0.04						
35.06±0.04						
40.04±0.05	3.637 ±0.011	4.597 ±0.019	4.857 ±0.025	5.326 ±0.020	11.49 ±0.07	12.13 ±0.06
45.01±0.06						
50.08±0.08	1.967 ±0.005	2.469 ±0.012	2.592 ±0.012	2.880 ±0.012	6.156 ±0.030	6.551 ±0.040
55.04±0.10						
60.03±0.12	1.207 ±0.003	1.534 ±0.003	1.580 ±0.002	1.761 ±0.008	3.779 ±0.011	4.072 ±0.013
61.82±0.12						
70.04±0.16	0.8110±0.0023	1.004 ±0.004	1.055 ±0.003	1.163 ±0.006	2.447 ±0.004	2.688 ±0.015
70.20±0.16						
79.96±0.21	0.5920±0.0018					
80.16±0.22						
84.99±0.23		0.6319±0.0027	0.6604±0.0033	0.7057±0.0034	1.442 ±0.006	1.582 ±0.004
89.92±0.26	0.4542±0.0015					
90.18±0.26						
94.00±0.28						
100.06±0.32	0.3674±0.0018	0.4304±0.0066	0.4550±0.0020	0.4852±0.0026	0.9456±0.0054	1.042 ±0.004
100.38±0.33						
109.99±0.39	0.3085±0.0010					
110.39±0.39						
114.87±0.43		0.3244±0.0026	0.3410±0.0020	0.3716±0.0022	0.6798±0.0043	0.7454±0.0038
120.21±0.47	0.2661±0.0020					
120.67±0.47						
123.09±0.49						
127.11±0.53						
130.31±0.55	0.2374±0.0016	0.2658±0.0018	0.2802±0.0023	0.2963±0.0027	0.5179±0.0028	0.5762±0.0045
131.41±0.55						

TABLE I (*continued*)

X-ray energy (keV)	Molybdenum (cm^2/gm)	Silver (cm^2/gm)	Tin (cm^2/gm)	Lanthanum (cm^2/gm)	Gadolinium (cm^2/gm)	Hafnium (cm^2/gm)
24.00±0.02		10.94 ±0.08				
25.00±0.02	44.35 ±0.24	9.818 ±0.042	11.49 ±0.07	17.25 ±0.09	23.83 ±0.16	34.51 ±0.21
26.01±0.02		53.95 ±0.37				
28.00±0.02			8.251 ±0.030			
30.04±0.03	27.30 ±0.15	36.36 ±0.18	41.71 ±0.22	10.25 ±0.05	15.35 ±0.08	21.37 ±0.18
35.05±0.04						
35.06±0.04				6.835±0.038	9.926±0.106	13.96 ±0.15
40.04±0.05	12.91 ±0.06	17.09 ±0.06	19.13 ±0.08	27.06 ±0.18	6.949±0.027	9.85 ±0.10
45.01±0.06					5.107±0.027	
50.08±0.08	7.034 ±0.036	9.231 ±0.036	10.53 ±0.03	14.44 ±0.06		5.378±0.036
55.04±0.10					15.43 ±0.10	
60.03±0.12	4.320 ±0.012	5.708 ±0.026	6.522 ±0.030	8.963±0.055	12.41 ±0.07	3.341±0.014
61.82±0.12						
70.04±0.16	2.804 ±0.014	3.786 ±0.025	4.271 ±0.026	5.961±0.027	8.180±0.039	10.45 ±0.07
70.20±0.16						
79.96±0.21		2.636 ±0.016		4.161±0.022	5.687±0.046	7.449±0.049
80.16±0.22						
84.99±0.23	1.666 ±0.009		2.525 ±0.010			
89.92±0.26		1.934 ±0.008		3.071±0.014	4.165±0.030	5.424±0.058
90.18±0.26						
94.00±0.28						
100.06±0.32	1.097 ±0.008	1.454 ±0.004	1.676 ±0.012	2.319±0.011	3.127±0.022	4.203±0.029
100.38±0.33						
109.99±0.39						3.271±0.034
110.39±0.39						
114.87±0.43	0.7840±0.0027	1.036 ±0.008	1.172 ±0.003	1.638±0.007	2.229±0.009	
120.21±0.47						2.557±0.042
120.67±0.47						
123.09±0.49						
127.11±0.53						
130.31±0.55	0.6299±0.0023	0.7524±0.0032	0.8476±0.0057	1.184±0.009	1.575±0.016	2.176±0.035
131.41±0.55						

X-ray energy (keV)	Tungsten (cm^2/gm)	Gold (cm^2/gm)	Lead (cm^2/gm)	Thorium (cm^2/gm)	Uranium (cm^2/gm)	Plutonium (cm^2/gm)
24.00±0.02						
25.00±0.02	35.96 ±0.25	43.48 ±0.18	50.78 ±0.58	60.62 ±0.32	63.75 ±0.48	67.5 ±1.3
26.01±0.02						
28.00±0.02						
30.04±0.03	22.61 ±0.27	26.86 ±0.08	31.60 ±0.21	38.04 ±0.30	41.08 ±0.27	42.98 ±0.64
35.05±0.04					28.32 ±0.16	
35.06±0.04						
40.04±0.05	10.45 ±0.12	12.79 ±0.09	14.90 ±0.14	18.03 ±0.07	19.60 ±0.11	21.77 ±0.20
45.01±0.06						
50.08±0.08	5.746±0.036	6.996±0.024	7.948±0.031	10.12 ±0.05	11.15 ±0.05	11.70 ±0.15
55.04±0.10						
60.03±0.12	3.623±0.023	4.365±0.020	4.875±0.020	6.487±0.019		7.40 ±0.10
61.82±0.12					6.476±0.022	
70.04±0.16		2.892±0.018	3.251±0.016	4.298±0.025		4.953±0.081
70.20±0.16					4.670±0.035	
79.96±0.21	7.729±0.028		2.318±0.009	3.101±0.014		3.543±0.024
80.16±0.22					3.397±0.028	
84.99±0.23		7.602±0.061				
89.92±0.26	5.816±0.035	6.590±0.040		2.284±0.009		2.594±0.016
90.18±0.26					2.446±0.026	
94.00±0.28			6.462±0.025			
100.06±0.32	4.362±0.037	5.032±0.016		1.761±0.008		1.956±0.014
100.38±0.33					1.918±0.011	
109.99±0.39			4.327±0.020			1.553±0.012
110.39±0.39					1.507±0.015	
114.87±0.43	3.166±0.018	3.588±0.016		4.725±0.027		
120.21±0.47				4.266±0.033		
120.67±0.47					4.277±0.041	
123.09±0.49					4.245±0.022	
127.11±0.53					3.870±0.024	
130.31±0.55	2.322±0.021	2.635±0.024	2.878±0.018	3.516±0.018	3.84 ±0.12	3.718±0.035
131.41±0.55					3.618±0.036	

From this foil a uniformly thick portion of the sample having an area of approximately 1 sq. in. was trimmed. The area and weight of this sample were then measured, and its average thickness in gm/cm^2 was calculated. The sample was then mounted in a foil holder which permitted it to be positioned normal to the diffracted beam (see Fig. 1). The sample could be moved with respect to the beam so that any part of it could be exposed to the x rays. Errors introduced by deviations from the average thickness of the sample were then minimized by measuring the transmission at a large number of positions over the foil area.

Thicker samples were machined to the shape of cylinders. The uniformity of the thickness of these machined samples was usually better than 0.1%.

Four Pu samples were fabricated by lapping disks machined from a Pu rod to foils of thicknesses of 0.001, 0.002, 0.005, and 0.010 in. The Pu foils were clad with 0.0004-in. Ni foils for health protection. The thickness of the thin Pu foil varied over its area by about 20%. The nonuniformity of the thin Pu foils introduced sizable errors in the measured Pu attenuation coefficients for the lower energies.

A specimen from each batch of material used for preparing the samples for each element was subjected to a chemical analysis for the purpose of determining the quantities of all impurities in the samples. In general the samples were very pure, but for some elements small corrections had to be applied to the measured attenuation coefficients because of impurities.

EXPERIMENTAL PROCEDURE

In addition to the sample thickness, three numbers are needed to calculate μ, namely, the incident-beam intensity, the attenuated-beam intensity, and a background correction. Count rates in the NaI counter varied from 3500 counts/min at 25 keV and 130 keV to 50 000 counts/min at 60 keV. Counting times of 1 min were used for each of the counts in the following sequence: background, no sample, sample, sample, sample, no sample, background, no sample, sample, $\cdots$. The sequence was continued for a given x-ray energy in most cases until counting statistics contributed less than 0.5% error to the measured value of μ. The number of "sample" counts varied from 6 to 24. The sample was moved after each sample count in order to average out variations from the average foil thickness. Because of the lower count rates at 25 and 130 keV, 2 min counting times were used for these energies. The background count was taken by placing a $\frac{1}{4}$-in. piece of lead in the sample position in the diffracted beam. Most efficient use of counting time was made by selecting a sample which gave a value of I/I_0 in the range of $0.1<I/I_0<0.4$ for a given x-ray energy. For many of the data points, two or more foils of different thicknesses were used to measure the attenuation coefficients. In every case the measured values were the same, within experimental error. For the heavier elements, as many as seven foils of different thicknesses were used to measure μ over the energy range of interest. These facts suffice to demonstrate that the experimental arrangement yields an exponential dependence of transmittance on absorber thickness and that a correct measure of μ is being made. For the radioactive foils Th, U, and Pu, foil and room background counts were taken with the x-ray machine turned off in order to make the necessary corrections in calculating μ. In taking the Pu data, the "no sample" counts were taken with two layers of 0.0004-in. Ni in the beam to correct for the attenuation caused by the Ni cladding on the Pu foils.

DATA ANALYSIS

From the sequence of counts taken for a given x-ray energy, a series of transmission ratios ($R=I/I_0$) were calculated. The procedure was as follows. Let the sequence of counts be denoted by B_1, N_1, S_1, S_2, S_3, N_2, B_2, N_3, S_4, S_5, $\cdots$ where B is a background count, N is a no-sample count, and S is a sample count (all counts are for the same counting time). Then

$$\begin{aligned} R_1&=(S_1-B_1)/(N_1-B_1)\\ R_2&=(2S_2-B_1-B_2)/(N_1+N_2-B_1-B_2)\\ R_3&=(S_3-B_2)/(N_2-B_2)\\ R_4&=(S_4-B_2)/(N_3-B_2)\\ R_5&=(2S_5-B_2-B_3)/(N_3+N_4-B_2-B_3)\\ &\vdots \end{aligned} \tag{2}$$

In this manner a set R_i was calculated for a given sample for a given energy. From the mean ($\bar{R}$) of the set, a value of the attenuation coefficient (μ) was calculated as follows

$$\mu=-x^{-1}\ln\bar{R}, \tag{3}$$

where x=average sample thickness in gm/cm^2.[8] When more than one sample was used at a given energy, a weighted average of the results from each sample was calculated. From the standard deviation (ΔR) calculated from the set R_i, a standard deviation in the attenuation coefficient ($\Delta\mu$) was calculated. For the radioactive samples, a foil correction factor C_f was subtracted from the numerator of each R_i where

$$C_f=(\text{foil background}—\text{room background})$$

with the x-ray machine off. These counts were taken for a long period of time and corrected to the proper counting time. The values of C_f were different for each x-ray energy because of different settings on the single-channel analyzer. The foil correction factors were less than 1% for U and Th. For Pu, C_f varied between 1% and 30% of the sample count. These calculations were all performed by an IBM 7094 digital computer.

[8] In the plutonium experiment, because the variations in the individual measurements of R_i were mainly due to differences in foil thickness rather than counting statistics, the attenuation coefficient at each energy was calculated from $\mu=-x^{-1}\langle\ln R_i\rangle_{\text{av}}$ rather than from $\mu=-x^{-1}\ln\langle R_i\rangle_{\text{av}}$.

From the chemical quantitative analysis of each sample, corrections in μ because of impurities were applied as follows:

$$\mu_{\text{element}}=(\mu_{\text{meas}}-\sum_i \mu_i f_i)/(1-\sum_i f_i) \qquad (4)$$

where μ_i is the attenuation coefficient for the ith impurity element and f_i is the weight fraction of ith impurity element in the sample. Since the values of f_i were small, accurate values of μ_i were not required. Impurity corrections ranged from zero for most elements to 12% for Be at 25 keV.

Some of the light element samples were as long as 0.9 in. For the lower energy x rays, attenuation by this length of air is not negligible. Thus, air-attenuation corrections were applied to the low-energy Be and C data. These corrections were of the order of 0.1%.

The wavelength of the diffracted radiation was calculated from the Bragg relationship

$$n\lambda=2d\sin\theta, \qquad (5)$$

where n was in every case unity. Wavelength was converted to energy by the formula[9]

$$E(\text{keV})\times\lambda(\text{Å})=12.3978. \qquad (6)$$

The energy error was calculated from the uncertainty in the Bragg angle, whose upper limit is ± 1 min. The energy error is in every case less than 1%.

RESULTS

The results of the present series of measurements are listed in Table I. The indicated errors are one standard deviation.

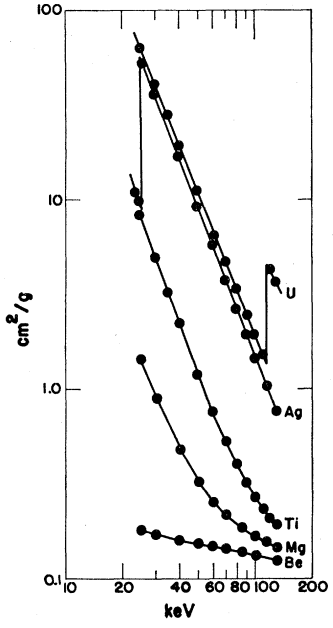

FIG. 2. Attenuation coefficients (cm²/gm) versus x-ray energy (keV) for Be, Mg, Ti, Ag, and U.

[9] E. R. Cohen and J. W. M. DuMond, Rev. Mod. Phys. 37, 561 (1965).

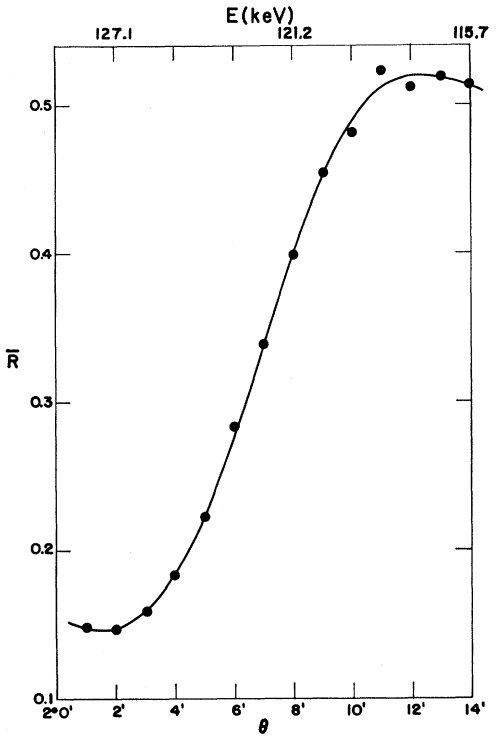

FIG. 3. Plutonium K edge.

The attenuation coefficients of five representative elements (Be, Mg, Ti, Ag, and U) are plotted in Fig. 2. The present work is in excellent agreement with the results of Deslattes[10] over the small energy region (25–30 keV) where the two overlap. The same applies to the recent work of Bearden.[11] Here the overlapping energy region is from 25 to 40 keV for four elements.

A separate experiment was performed with a 0.010-in. Pu foil in which the Pu K edge energy was measured. An energy sweep was made over the vicinity of the Pu K edge by changing the Bragg angle by 1′ intervals and measuring the fraction of the x rays transmitted through a given spot on the 0.010-in. Pu foil. The results are shown in Fig. 3. The Pu K edge was observed at 122.2 ± 0.5 keV (one standard deviation) which is in agreement with the Cauchois[12] value of 121.75 keV.

ERRORS

Sources of random errors include counting statistics, variations in x-ray beam intensity, uncertainties in sample thickness, and errors in applying sample impurity corrections. Counting statistics for most of the measurements were less than 0.5%. Errors due to variations in beam intensity and sample thickness

[10] R. D. Deslattes, U. S. Air Force Office of Scientific Research Report No. AFOSR-TN-58-784, 1958 (unpublished).

[11] Alan J. Bearden, J. Applied Phys. 37, 1681 (1966).

[12] Y. Cauchois, J. Phys. Radium 13, 113 (March 1952).

were kept to a minimum by the data-taking sequence and the number of individual measurements made of μ. An indication of the size of these errors is given by the standard deviations in Table I. Since the sample impurity corrections are small, the errors in this correction are believed to be quite small. The only possible exception to this is the Be data where the impurity correction varies from zero to twelve percent. Errors in the Be attenuation coefficients are believed to be less than 2%. There are no known sources of systematic errors in the present work.

ACKNOWLEDGMENTS

The authors express their appreciation for the many helpful discussions with Prof. G. B. Arfken, Miami University, Oxford, Ohio. They also acknowledge the assistance of J. R. Brown who wrote the computer program used in analyzing the data.

PHYSICAL REVIEW VOLUME 153, NUMBER 2 10 JANUARY 1967

Relaxation of OH^- Dipoles in KCl at Low Temperatures*

LAWRENCE A. VREDEVOE†
University of California, Los Angeles, California
(Received 11 April 1966; revised manuscript received 23 June 1966)

The direct and Raman relaxation rates of OH^- electric dipoles in KCl are computed using a point-charge–point-dipole model in which we allow for the possibility that the equilibrium position of the dipole is displaced from the center of octahedral symmetry. This model can thus include the effect of an OH^- quadrupole moment. Such a moment can be represented by an effective displacement of the dipole. Estimates are made of the rates at temperatures between 2 and 11°K in the presence of weak and strong dc electric fields parallel to the [001] or [111] axis. Our estimates are in good agreement with the value measured by Feher, Shepherd, and Shore at 11°K. Agreement with the rate measured by Bron and Dreyfus at 1.4°K is obtained by allowing for an effective displacement of the dipole equilibrium position from a centrosymmetric position. The Raman transitions are shown to be strongly temperature-dependent, dominating the dipole-lattice relaxation processes at very low temperatures, while the direct transitions display a linear temperature dependence.

I. INTRODUCTION

In this paper we examine the phonon-induced relaxation of OH^- electric dipoles in low-temperature KCl crystals with a dc electric field applied parallel to either the [001] or [111] axis. Recent para-electric-resonance experiments by Feher, Shepherd, and Shore[1] have suggested that, for a 15.1 kV/cm dc electric field parallel to the [111] axis, this dipole-lattice relaxation rate is of order 10^{11} sec^{-1} at 11°K. Bron and Dreyfus[2] have estimated from the linewidth of the microwave resonance absorption in the presence of a weak [001] dc electric field that at 1.4°K the dipole-lattice relaxation rate is 3×10^8 sec^{-1}, a value which is in substantial agreement with the measurements of others.[3,4]

We use a point-charge–point-dipole model. The phonon electric field of the nearest-neighbor cluster is expanded in a power series in the local strains and their derivatives. The interaction of this field with the OH^- dipole is calculated. We also include the first-order terms arising from displacement of the dipole equilibrium position from the center of octahedral symmetry. That displacements of this kind can occur has been suggested by Bron and Dreyfus[2] for OH^-:KCl and Lombardo and Pohl[5] for Li-doped alkali halides. It is a well-known theorem of electrostatics that displacement of a point dipole is equivalent to superimposing a quadrupole moment on the dipole at its original position. The presence of the OH^- quadrupole moment can therefore be considered as equivalent to an effective dipole displacement. In our final estimate for the relaxation rate, we shall therefore be unable to distinguish between these two effects. We shall show that the measured relaxation rates in the low-temperature (helium) range can be accounted for only by allowing for such displacements. Our treatment will be limited to the direct and Raman terms of the phonon field because these terms dominate the relaxation at low temperatures.

Since OH^- is a light defect, the effect of the mass perturbation in the absence of changes in bonding will give rise to localized modes above the acoustic band.[6]

* Supported in part by the National Science Foundation and Office of Naval Research, Contract No. NONR 233(88).
† National Aeronautics and Space Administration Predoctoral Fellow.
[1] G. Feher, I. Shepherd, and H. Shore, Phys. Rev. Letters **16**, 500 (1966).
[2] W. Bron and R. Dreyfus, Phys. Rev. Letters **16**, 165 (1966).
[3] U. Kuhn and F. Luty, Solid State Commun. **4**, 31 (1965).
[4] U. Bosshard, R. Dreyfus, and W. Kanzig, Phys. Kondensierten Materie **4**, 254 (1965).
[5] G. Lombardo and R. Pohl, Phys. Rev. Letters **15**, 291 (1965).
[6] P. Dauber and R. Elliott, Proc. Roy. Soc. (London) **A273**, 222 (1963).